Polym. Bull. (2011) 67:321–331
DOI 10.1007/s00289-011-0478-z

ORIGINAL PAPER

Nonisothermal crystallization behavior and UV screening ability of poly(ethylene terephthalate)/carbon black transparent films

Qilin Zhou · Yue Zhang · Qiuying Li · Chifei Wu

Received: 15 September 2010 / Revised: 17 February 2011 / Accepted: 29 March 2011 /
Published online: 27 May 2011

Abstract A UV absorbent was blended with virgin carbon black to prepare modified carbon black (m-CB) using a solid phase modification. The mixed solutions of poly(ethylene terephthalate) (PET)/CB and PET/m-CB were coated on glass substrates to fabricate light screening films. Scanning electron microscopy (SEM) showed that m-CB had better dispersibility than CB in PET matrix. Nonisothermal crystallization kinetics of virgin PET, PET/CB, and PET/m-CB films were investigated by differential scanning calorimetry (DSC). The data were described by a modified Avrami model. The results showed CB and m-CB acted as nucleating agents and increased the crystallization rate of PET. But due to the low crystallization capacity of copolymerized PET (co-PET) matrix, the nucleating effects were not as obvious as expected. The addition of 4 wt% m-CB improved the UV screening ability of the composite film significantly and just slightly increased their haze.

Keywords Poly(ethylene terephthalate) · Carbon black · UV327 · Crystallization

Introduction

Nowadays, poly(ethylene terephthalate) (PET) has a variety of applications such as fibers, bottles, films, and engineering plastics in automobiles and electronics [1]. PET film is one of the most important applications of PET. In order to prepare conductive transparent films, gas barrier films or solar films, it is usually combined with other materials to obtain different properties. The transparency of polymer film is mainly influenced by the crystallization and the spherulite size of polymer [2]. Research on the crystallization of PET was popular in the last 20 years. Recently a great progress has

Q. Zhou · Y. Zhang · Q. Li · C. Wu (✉)
Polymer Alloy Laboratory, School of Materials Science and Engineering, East China University of Science and Technology, 130 Meilong Road, Shanghai 200237, People's Republic of China
e-mail: wucf@ecust.edu.cn

been made in PET nanocomposites. Homogeneous dispersion of inorganic nanoparticles in a PET matrix can improve its properties. However, crystallization mechanism of PET nanocomposites is very complicated. Many researchers have made great efforts to explain the crystallization kinetics of PET nanocomposites.

Carbon black (CB) is an efficient nucleating agent [3]. This behavior has been observed in other polymer/CB systems, such as polypropylene (PP)/CB [3–5], polyvinylidene fluoride (PVDF)/CB, and polyamide (PA)/CB [6]. But CB can aggregate easily, so it cannot be dispersed in polymer matrix homogeneously. To improve the dispersion ability of CB in polymer systems, grafting polymers or organic molecules onto the CB surface is known to be one of the effective methods. Li et al. [7] reported the modification of CB by trapping long chain radicals of poly(vinyl alcohol) (PVA) formed by sonochemical degradation. Akovali and Ulkem [8] and Tricas et al. [9, 10] reported the modification of CB by plasma polymerization. However, most of the above approaches were conducted in liquid phase, leading to inconvenient process. Yang et al. [11] reported the modification of carbon black by introduction of hydroxy methyl groups through the reaction between unsaturated hydrogen atoms of the polycondensed aromatic rings of carbon black and formaldehyde under alkali conditions. In our former study, a simple non-liquid-phase approach was used to fabricate organically modified CB (m-CB) by blending a commercial CB (N220) and a low-molecular-weight organic compound (AO-80) in a rheology mixer [12]. The m-CB had a smaller particle size than the virgin CB, and it could be dispersed easily in acetone to form a stable suspension. In the present study, a commercial UV absorbent 2-(2′-hydroxy-3′,5′-di-*tert*-butyl-phenyl)-5-chlorobenzotriazole (UV327) was used to blend with CB to increase the UV absorption ability of CB. Moreover, the prepared m-CB could be dispersed stably in polar solvent, leading to uniform dispersion in a PET matrix. The nonisothermal crystallization kinetics of virgin PET film and PET nanocomposite films were studied by a modified Avrami model. The effect of m-CB on the crystallization and UV screening ability of PET film is reported in this article.

Experimental

Materials and methods

The CB used was pigment black Mogul-L provided by Cabot Corp., USA. PET (F51 M) was provided by Toray Corp., Japan. UV327 was bought from Hangzhou Shinyang Samwoo Fine Chemical Co., Ltd., China. The chemical structure of UV327 is shown in Fig. 1.

The virgin CB was first dried in a vacuum oven at 105 °C for 24 h to remove the adsorbed water. The m-CB was prepared by mixing virgin CB and UV327 together at a 50/50 (wt/wt) ratio in a Rheomix 600p internal mixer (Haake, Germany) for 20 min with a starting temperature of 160 °C. Two counter-rotating σ-type rollers ran at a speed of 60 rpm.

The virgin PET, PET/CB, PET/UV327, and PET/m-CB films were formed on 4 mm thickness glass substrates in the following process: first, a certain amount of

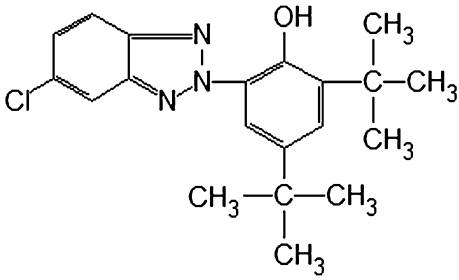

Fig. 1 Chemical structure of UV327

PET was dissolved in 50/50 (vol/vol) phenol/tetrachloroethane solvent at 80 °C; second, CB, UV327, or m-CB were added into the obtained solution during ultrasonic dispersion; third, the mixed solution (1.5 mL) was dropped on a glass substrate and coated using a spiral bar coater; fourth, the glass substrates with films were dried in a vacuum oven at 45 °C for 12 h to remove phenol/tetrachloroethane solvent.

Characterization

Scanning electron microscopy (SEM)

PET/CB and PET/m-CB composite films with different content of CB and m-CB were freeze-fractured in liquid nitrogen, and the fractured surfaces were then gold-sputtered in vacuo before they were observed in a JEOL JSM-5410 scanning electron microscope (Japan) with a working voltage of 15 kV.

Differential scanning calorimeter (DSC)

Differential scanning calorimeter (DSC) was performed on Netzsch DSC PC 200 (Germany). The sample (7–10 mg) was initially heated to 250 °C, and held for 10 min in order to remove prior thermal history. Then it was cooled to 80 °C at 2.5, 5, 10, or 15 °C/min, respectively. The crystallization parameters, the temperature of the exothermal peak (T_c), and the temperature of the onset of crystallization (T_o) were obtained from the cooling scans.

Ultraviolet and visible spectrophotometry (UV–vis)

Optical transmittance in the UV–vis range of the samples was measured by a UV–vis spectrophotometer (Cary 5000, Varian, USA). Haze of the samples was calculated.

Results and discussions

Dispersibilities of CB and m-CB in PET

Figure 2 shows the cryofractured surface of PET/CB and PET/m-CB films observed by SEM. It can be seen in Fig. 2a that primary particles of CB fuse together to form

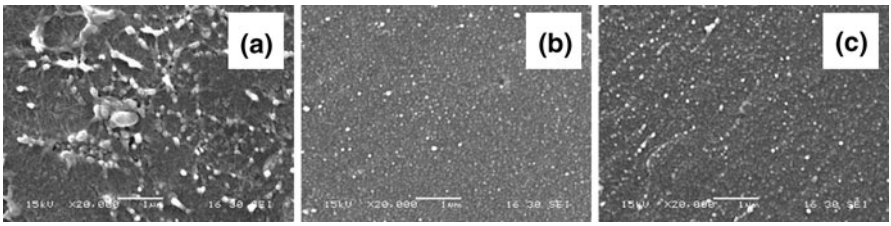

Fig. 2 SEM micrographs of PET films with **a** 2 wt% CB, **b** 2 wt% m-CB, **c** 4 wt% m-CB

aggregates. Compared with Fig. 2a, m-CB exhibited a finer distribution in the PET film, as shown in Fig. 2b and c. Moreover, m-CB keeps fine and stable dispersion when the content of m-CB increased from 2 to 4 wt%. After the modification of CB with UV327, the surface of m-CB becomes more lipophilic which makes it disperse more uniformly in a PET matrix. This result also proves that in situ modification of CB is an efficient method to prepare m-CB.

Non-isothermal crystallization process

The non-isothermal crystallization processes of PET film, and PET with 2 wt% CB, PET with 2 wt% UV327, and PET with 4 wt% m-CB composite films from the melt were measured at various cooling rates from 2.5 to 15 °C/min. The DSC curves of all the samples are presented in Fig. 3. The nonisothermal crystallization parameters: ΔH_c crystallization enthalpy, T_o the onset temperature of crystallization, T_c the exothermic peak temperature of crystallization, and $t_{1/2}$ half crystallization time were determined from these curves and the results are listed in Table 1. Obviously, the exothermic peaks shifted to lower temperature as the cooling rate increased. For a given cooling rate, compared with those for virgin PET, T_o and T_c for PET/CB, PET/UV327 and PET/m-CB shifted to higher temperature. $t_{1/2}$ shows that the crystallization rates of PET/CB, PET/UV327, and PET/m-CB were higher than the virgin PET, indicating that CB, UV327, and m-CB can act as nucleating agents for the PET matrix. On the other hand, compared with CB and UV327, m-CB was a more efficient nucleating agent. Therefore, PET crystallized at higher temperature in the PET/m-CB film than in the PET/CB and PET/UV327 films, and the crystallization rate of PET/m-CB was higher than the other two samples. This can be explained by the better dispersibiliy of m-CB than virgin CB. The combination of CB and UV327 helps m-CB to disperse homogeneously in the PET matrix and performs as a more efficient nucleating agent for PET.

In the nonisothermal crystallization process, the relative crystallinity $X(t)$, a function of crystallization temperature T, can be formulated as

$$X(t) = \int_{T_o}^{T} \left(\frac{dH_c}{dT}\right) dT \Big/ \int_{T_o}^{T_\infty} \left(\frac{dH_c}{dT}\right) dT \quad (1)$$

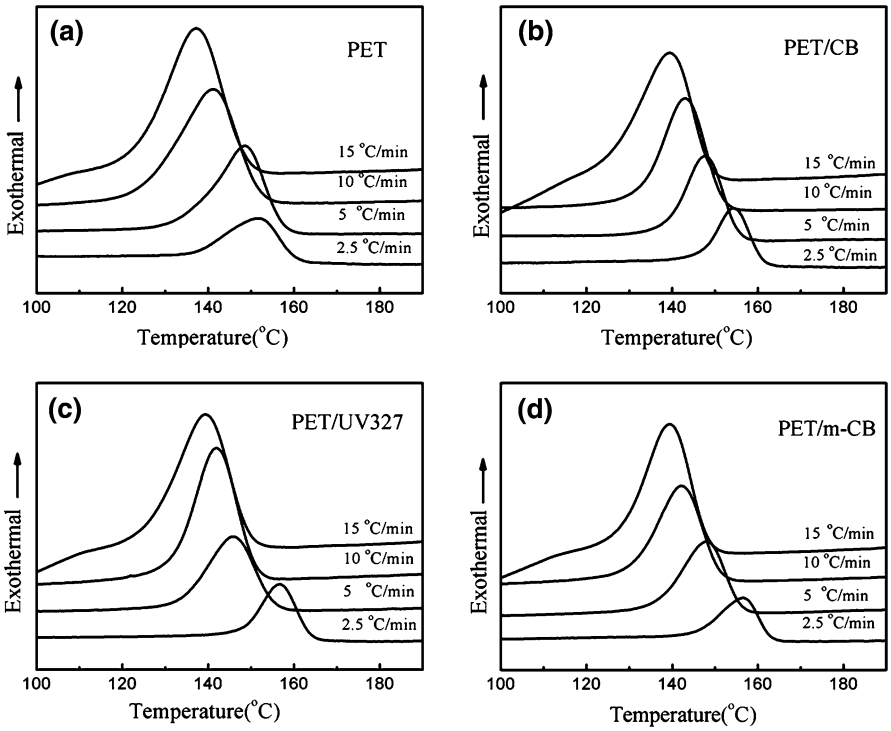

Fig. 3 DSC curves of virgin PET, PET/2 wt% CB, PET/2 wt% UV327, and PET/4 wt% m-CB in the crystallization process from the melt at various cooling rate from 2.5 to 15 °C/min

where T_o and T_∞ represent the temperatures at the onset and the end of the crystallization process, respectively, and dH_c is the enthalpic heat of crystallization released during an infinitesimal temperature range dT [13].

The crystallization time (t) can be calculated by the following equation:

$$t = (T_o - T)/|\beta| \tag{2}$$

where T is the temperature at time t and β is the cooling rate.

Figure 4 shows the plots of the relative crystallinity $X(t)$ versus crystallization time t. The half-time of crystallization ($t_{1/2}$) can be determined from these curves and is summarized in Table 1. $t_{1/2}$ decreased as the cooling rate increased, indicating that the crystallization of PET was faster at a higher cooling rate. Compared to that of PET/CB composite films, $t_{1/2}$ of PET/m-CB was lower at the same cooling rate. Therefore, the crystallization rate of PET/m-CB composite film was higher than PET/CB composite film. In general, there are two mutually opposite effects of CB on the crystallization behavior: nucleating ability and growth retardation, both of which are related to the content and dispersion state of CB. Compared to PET composite films with 2 wt% CB, the addition of 4 wt% m-CB increased the number of nucleating agents and promoted the nucleating ability of PET. On the other hand, the modification of CB with UV327 improved the

Table 1 Crystallization parameters of virgin PET, PET/CB, PET/UV327, PET/m-CB composites

Sample	Cooling rate (°C/min)	ΔH_c (J/g)	T_o (°C)	T_c (°C)	$t_{1/2}$ (min)
PET	2.5	13.18	159.7	151.8	3.16
	5	12.50	157.0	148.6	1.68
	10	12.75	151.2	141.4	0.98
	15	13.01	148.3	137.1	0.75
PET/CB 98/2	2.5	17.31	160.8	154.4	2.56
	5	16.32	155.2	147.4	1.56
	10	15.69	151.6	143.1	0.85
	15	15.92	148.7	139.4	0.62
PET/UV327 98/2	2.5	16.25	163.8	156.7	2.84
	5	15.97	154.7	145.8	1.78
	10	15.03	150.9	141.9	0.90
	15	14.26	149.2	139.2	0.67
PET/m-CB 96/4	2.5	15.82	162.7	156.3	2.52
	5	16.31	155.7	148.4	1.46
	10	16.89	150.6	142.1	0.85
	15	16.12	148.2	139.3	0.59

dispersibility of m-CB in PET film and made m-CB perform as a more effective nucleating agent for PET.

Nonisothermal crystallization kinetics

Avrami equation [14] is often used to analyze isothermal crystallization kinetics

$$1 - X(t) = \exp(-Zt^n) \tag{3}$$

where $X(t)$, Z, and n denote the relative crystallinity at the time t, the crystallization rate constant and the Avrami exponent which describes the mechanism of crystallization, respectively. Equation 3 can be transformed to Eq. 4.

$$\log[-\ln(1 - X(t))] = \log Z + n\log t \tag{4}$$

When the process is nonisothermal, Jeziorny [15] suggested that the rate parameter Z should be corrected for the influence of cooling rate β of the polymer, as the following:

$$\log(Z_c) = (\log Z)/\beta \tag{5}$$

where Z_c is the revised crystallization rate constant.

Figure 5 shows the plots of $\log[-\ln(1 - X(t))]$ versus $\log t$ for virgin PET, PET/CB, PET/UV327, and PET/m-CB composites at various cooling rates. Each plot has a linear portion in the early stage of crystallization progress. As expected, modified Avrami equation can be applied to the PET/CB system to some extent. Consequently, Z and n can be calculated from the linear parts. The result is different

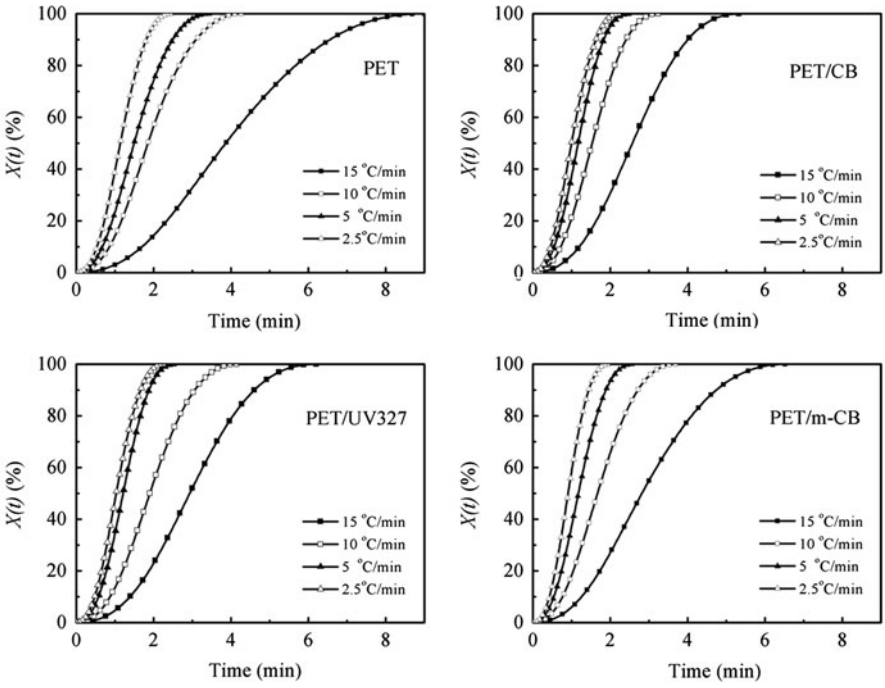

Fig. 4 Plots of $X(t)$ versus crystallization time at different cooling rates

from some reports which have indicated that Jeziorny method could not suit the PET/CB system properly. The reason we suggest is the difference between homo-PET and co-PET. Compared to homopolymerization system, this co-PET which is suitable for film application cannot crystallize easily. Therefore, although CB, UV327, or m-CB had a great nucleating effect, the crystallization kinetics of PET/CB, PET/UV327 and PET/m-CB composites can still described by the modified Avrami method.

n and Z_c for virgin PET, PET/CB, PET/UV327, and PET/m-CB calculated from the linear parts of Fig. 5 are collected in Table 2. The values of n for virgin PET range from 2.28 to 2.38, indicating that the crystal growth was between two-dimensional and three-dimensional with homogeneous nucleation. With the addition of CB, UV327, or m-CB, the values of n increased a little. This implies that their spherulite growth was similar to that of virgin PET. Moreover, Z_c for PET/CB and PET/m-CB was a little higher than that of virgin PET at the same cooling rate, indicating that the crystallization rate of PET/CB and PET/m-CB did not increase very much, which is in agreement with the results of $t_{1/2}$. It has been reported that CB and m-CB can significantly influence the mechanism of nucleation and crystal growth of PET [16–19]. But in this co-PET system, crystallization capacity of co-PET was lower than that of homo-PET. Therefore, with the addition of CB and m-CB, crystallization capacity of the PET was not improved very much. As expected, this behavior of PET/CB and PET/m-CB composite is meaningful for preparing transparent PET films.

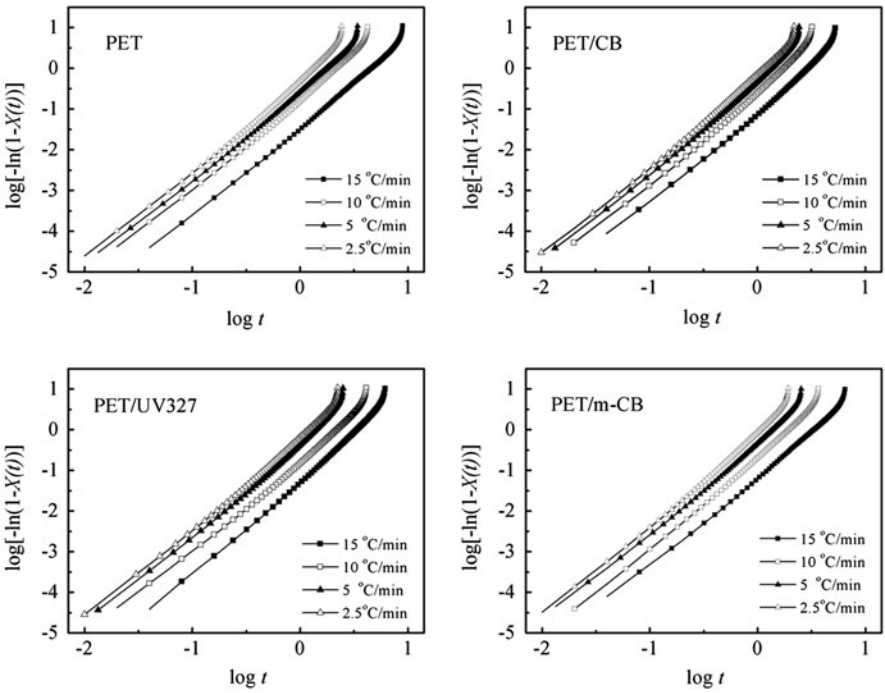

Fig. 5 Plots of $\log[-\ln(1 - X(t))]$ versus $\log t$ for nonisothermal crystallization of PET, PET/2 wt% CB, PET/2 wt% UV327, and PET/4 wt% m-CB composite films

Uvioresistant and transparent film

The transmittance of UV and visible light for PET and its composite films are shown in Fig. 6. The visible light and UV ray transmittance was very high for the virgin PET film. With the addition of CB, the transmittance of UV ray and visible light decreased simultaneously. But virgin CB just reduced the transmittance by physically screening UV and visible light. Therefore, the transmittance of UV and visible light was on the same level. As expected, PET/m-CB performs well in screening UV due to the addition of UV327 and the better dispersibility of m-CB. First, the benzotriazole group on the UV327 can effectively absorb the UV rays in the range of 300–400 nm. Second, the uniform dispersion and the smaller aggregates of m-CB benefit the transmittance of visible light.

Haze of the composite films was calculated to determine the transparency of the films. Haze is that percentage of the total transmitted light which, in passing through the specimen, is scattered from the incident beam by more than 2.5°. The haze (%) is measured in accordance with the procedures specified in ASTM D 1003-07.

$$\text{haze} = T_d/T_t \times 100\% \tag{6}$$

where T_d is the light scattered by specimen, and T_t is the total transmittance of incident light.

Table 2 Results of the Avrami analysis for nonisothermal crystallization of virgin PET, PET/CB, PET/UV327 and PET/m-CB composite films

Sample	Cooling rate (°C/min)	Z_c	n
PET	2.5	0.03	2.28
	5	0.17	2.32
	10	0.29	2.31
	15	0.56	2.38
PET/CB 98/2	2.5	0.08	2.39
	5	0.27	2.42
	10	0.53	2.42
	15	0.75	2.37
PET/UV327 98/2	2.5	0.05	2.35
	5	0.17	2.43
	10	0.49	2.37
	15	0.70	2.46
PET/m-CB 96/4	2.5	0.07	2.30
	5	0.22	2.38
	10	0.52	2.36
	15	0.96	2.41

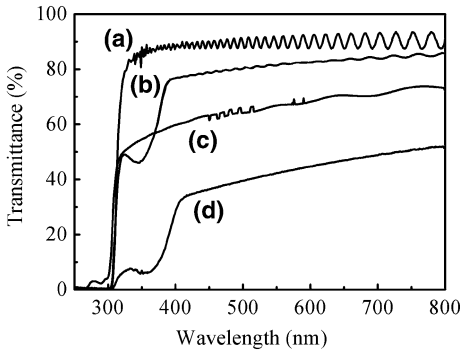

Fig. 6 UV and visible light transmittance of (*a*) virgin PET film, (*b*) PET/2 wt% UV327 composite film, (*c*) PET/2 wt% CB composite film, and (*d*) PET/4 wt% m-CB composite film

The average haze of visible light for the four samples is calculated and listed in Table 3. As shown, compared with virgin PET, the hazes of PET/CB, PET/UV327, and PET/m-CB composite films increased a little, suggesting CB, UV327, and m-CB do not influence the crystallization capacity of PET matrix very much. This result is also proved by the modified Avrami equation described above. The low haze for PET/m-CB film results in the fine definition for the composite film which with low vis transmittance.

Conclusions

The modification of CB by UV327 improves the dispersibility of CB is shown slightly by SEM. With the addition of CB and m-CB, PET composite films

Table 3 Average haze in the wavelength range from 400 to 800 nm for virgin PET and PET composite films

Sample	T_d (%)	T_t (%)	Haze (%)
PET	2.9	89.8	3.2
PET/CB	6.0	68.0	8.8
PET/UV327	5.3	80.3	6.6
PET/m-CB	3.7	43.9	8.4

crystallized faster than virgin PET film, indicating that CB and m-CB acted as nucleating agents and m-CB promoted the crystallization of PET matrix more effectively than virgin CB. As expected, the modified Avrami equation was suitable for describing PET/CB and PET/m-CB composite systems. The results showed that the crystallization rate of co-PET was accelerated by CB or m-CB slightly, due to the difficulty for the organization and arrangement of co-PET. Therefore, the hazes of the PET/CB and PET/m-CB were not increased while adding CB and m-CB. Furthermore, it is shown that PET/m-CB has the best UV screening ability to produce UV screening film.

Acknowledgments The authors sincerely acknowledge the financial assistance of National Natural Science Foundation of China (50733001), National Key Technology R & D Program of China (2008BAC46B10) and the opening fund (2010) of Engineering Research Center of Biomass Materials,Ministry of Education, Southwest University of Science and Technology, Mianyang, China.

References

1. Guo WH, Tang XW, Yin GR, Gao YJ, Wu CF (2006) Low temperature solid-state extrusion of recycled poly(ethylene terephthalate) bottle scraps. J Appl Polym Sci 102:2692–2699
2. Stein RS, Prud'Homme R (1971) Origin of polyethylene transparency. J Polym Sci B 9:595–598
3. Mucha M, Marszalek J, Fidrych A (2000) Crystallization of isotactic polypropylene containing carbon black as a filler. Polymer 41:4137–4142
4. Mucha M, Krolikowski Z (2003) Application of DSC to study crystallization kinetics of polypropylene containing fillers. J Therm Anal Calorim 74:549–557
5. Wiemann K, Kaminsky W, Gojny FH, Schulte K (2005) Synthesis and properties of syndiotactic poly(propylene)/carbon nanofiber and nanotube composites prepared by in situ polymerization with metallocene/MAO catalysts. Macromol Chem Phys 206:1472–1478
6. Del Rio C, Ojeda MC, Acosta JL (2000) Carbon black effect on the microstructure of incompatible polymer blends. Eur Polym J 36:1687–1695
7. Li QY, Wu GZ, Ma YL, Wu CF (2007) Grafting modification of carbon black by trapping macroradicals formed by sonochemical degradation. Carbon 45:2411–2416
8. Akovali G, Ulkem I (1999) Some performance characteristics of plasma surface modified carbon black in the (SBR) matrix. Polymer 40:7417–7422
9. Tricas N, Vidal-Escales E, Borros S, Gerspacher M (2003) Influence of plasma polymerised carbon black on the in-rubber properties of filled compounds. In: 16th conference of the international society of plasma chemistry, Taormina, Italy
10. Tricas N, Borros S, Schuster RH (2004) Carbon black modification by atmospheric pressure plasma. In: Proceedings of the Kautschuk–Herbst–Kolloquium, Hannover, Germany
11. Yang Q, Wang L, Xiang WD, Zhou J, Jiang G (2007) Modification of carbon black through grafting multihydroxyl hyperbranched polyether onto its surface. J Appl Polym Sci 103:2086–2092
12. Huang JF, Shen F, Li XH, Zhou XQ, Li BY, Xu RL, Wu CF (2008) Chemical modification of carbon black by a simple non-liquid-phase approach. J Colloid Interface Sci 328:92–97
13. Cebe P, Hong S (1986) Crystallization behavior of poly(etheretherketone). Polymer 27:1183–1192

14. Avrami M (1940) Kinetics of phase change. II. Transformation-time relations for random distribution of nuclei. J Chem Phys 8:212–224
15. Jeziorny A (1978) Parameters characterizing kinetics of nonisothermal crystallization of poly(ethylene-terephthalate) determined by DSC. Polymer 19:1142–1149
16. Bian J, Ye SR, Feng LX (2003) Heterogeneous nucleation on the crystallization poly(ethylene terephthalate). J Polym Sci B 41:2135–2144
17. Chae DW, Kim BC (2007) Effects of introducing silica particles on the rheological properties and crystallization behavior of poly(ethylene terephthalate). J Mater Sci 42:1238–1244
18. Kim JY, Park HS, Kim SH (2006) Unique nucleation of multi-walled carbon nanotube and poly(ethylene 2,6-naphthalate) nanocomposites during non-isothermal crystallization. Polymer 47:1379–1389
19. Li XH, Guo WH, Zhou QL, Xu SA, Wu CF (2007) Non-isothermal crystallization kinetics of poly(ethylene terephthalate)/grafted carbon black composite. Polym Bull 59:685–697